Botanical Studies (2012) 53: 97-104.



# Embryology of the lady's slipper orchid, *Paphiopedilum delenatii*: Ovule development

Yung-I LEE[1,*] and Edward C. YEUNG[2]

[1]*Botany Department, National Museum of Natural Science, No 1, Kuan-Chien Rd., Taichung, Taiwan*
[2]*Department of Biological Sciences, University of Calgary, Calgary, Alberta T2N 1N4, Canada*

(Received December 13, 2010; Accepted August 30, 2011)

**ABSTRACT.** *Paphiopedilum delenatii* is an endangered slipper orchid with delicate flowers that is native to Vietnam. An understanding of this plant species' reproductive biology is required for its effective propagation and conservation. *P. delenatii* has a bisporic pattern of embryo sac development with a six-celled number in a mature embryo sac. Prior to pollination, the nucellar filaments are present within the ovary. The archesporial cell at the tip of the nucellar filament differentiates into a megasporocyte fifteen days after pollination. As the megasporocyte matures, the nucleus becomes located at the micropylar end of the cell, resulting in an uneven distribution of the cytoplasm with the starch granules becoming more abundant at the chalazal end. After the first meiotic division, a distinct callose layer separates the micropylar dyad from the chalazal one. Soon after, a callose wall completely encloses the functional dyad at the chalazal end. As the functional dyad increases its size, the callose remains in the common wall separating the two dyads as well as in the chalazal end wall of the functional dyad. One notable finding of this study is the presence of cuticular material in the lateral walls of the mature embryo sac. The deposition of the cuticular material may serve to strengthen the fairly large embryo sac and helps to conserve water for the developing embryo after fertilization.

**Keywords:** Callose; Embryology; Lady's slipper orchid; Nile red; Ovule.

## INTRODUCTION

Meiotic division allows for the random assortment of parental genes; the union of parental genes upon a successful fertilization event enables the offspring to better adapt to the changing environment. The ovule contains a megasporocyte which undergoes meiosis and gives rise to a female gametophyte through the process of megasporogenesis and megagametogenesis. Hence, ovules are the source of female gametophytes and the progenitors of seeds in flowering plants (Relser and Fischer, 1993). In order to understand the reproductive process, the study of ovule development is indispensable (Yeung and Law, 1997). One of the unique features of ovule development in orchids is that ovules are usually not present at the time of pollination (Swamy, 1943; Wirth and Withner, 1959). The development of numerous ovules is triggered by pollination that usually takes several weeks to complete (Arditti, 1992, Yeung and Law, 1997). The prolonged period of ovule development and their overall abundance in orchids provide a good opportunity to study this process (Zhang and O'Neill, 1993).

The lady's slipper orchid, *Paphiopedilum,* is one of the more popular orchid genera in the world and is comprised of about 80 species, many of which occur in tropic and subtropical Asia (Cribb, 1998). Among *Paphiopedilum* species, *P. delenatii* , which is native to Vietnam, produces delicate pinkish flowers on compact plants (Averyanov et al., 2003). This species has attracted special interest because of its great horticultural value as potted plants and its use in breeding programs. Popular among orchid enthusiasts worldwide, *P. delenatii* is now endangered, due to its over-collection and habitat destruction. Information concerning the reproductive biology of this endangered *Paphiopedilum* species may improve the current methods used for its conservation and artificial propagation.

While the majority of orchids have a monosporic pattern of embryo sac development (Vij and Sharma, 1986), earlier studies indicate that *Cypripedium* and *Paphiopedilum* species follow a bisporic pattern (Duncan and Curtis, 1942; Carlson, 1945). Although the structural pattern of *P. delenatii* embryo development, from fertilization to seed maturity, was documented in a previous study (Lee et al., 2006), information concerning its ovule development is lacking. The objective of this study was to document the anatomical and histochemical changes of *P. delenatii* ovules during the course of megasporogenesis and megagametogenesis, leading to mature embryo sac formation. The observations also serve as a detailed case history of ovule development in a slipper orchid and add to the current literature.

*Corresponding author: E-mail: leeyungi@mail.nmns.edu.tw; Tel: 886-4-23226940 ext. 153; Fax: 886-4-23285320.

## MATERIALS AND METHODS

### Plant Materials

*Paphiopedilum delenatii* plants were grown in greenhouses at the National Museum of Natural Science, Taichung, Taiwan. To ensure a good fruit set, flowers (Figure 1A) were manually self-pollinated by transferring pollen onto the stigma of the same flower. Developing ovaries and fruits were harvested at regular intervals after pollination. Approximately 70 flowers were gathered for this study.

### Light Microscopy

Developing ovaries were collected, cut into 3 to 4 mm sections and fixed in 2.5% glutaraldehyde and 1.6% paraformaldehyde buffered with 0.05M phosphate buffer, pH 6.8, for 24 h at 4°C. After fixation, the sections were dehydrated in methyl cellosolve (BDH Chemicals) for 24 hours, followed by two changes of 100% ethanol for 24 hours each at 4°C. The samples were infiltrated gradually (3:1. 1:1, and 1:3 100% ethanol: Historesin, 24 h each) with Historesin (Leica Canada, Markham, Ontario), followed by two changes of pure Historesin. The tissues were then embedded according to Yeung (1999). Serial sections, 3 μm thick, were cut using a Ralph knife on a Reichert-Jung 2040 Autocut rotary microtome. Sections were stained with Periodic Acid-Schiff's (PAS) reaction for total carbohydrate and counter-stained with either 0.05% (w/v) toluidine blue O (TBO) in benzoate buffer for general histology or 1% (w/v) amido black 10B in 7% acetic acid for protein (Yeung, 1984). The sections were viewed and the images were captured digitally using a CCD camera (Cool Snap fx, Photometrics, Tucson, AZ) attached to a light microscope (Axioskop 2, Carl Zeiss AG, Germany).

### The detection of lipidic substances

The accumulation of cuticular substance was detected using Nile red as detailed in Lee et al. (2006). The Historesin embedded tissues were stained with 1 μg $ml^{-1}$ of Nile red (Sigma Chemical Co., St. Louis, Mo.) for 10 min, briefly washed in distilled water, and mounted in water containing 0.1% n-propyl gallate (Sigma Chemical Co.), an antifading compound. The fluorescence pattern was examined using an epifluorescence microscope (Axioskop 2, Carl Zeiss AG) equipped with the Zeiss filter set 15 (546/12 nm excitation filter and 590 emission barrier filter).

### Callose determination

After fixation and ethanol dehydration, developing ovules were transferred into a clearing solution of lactic acid (85-92%, Wako Pure Chemical Industries) saturated with chloral hydrate for 24 h. The samples were washed and stained with 1% water-soluble aniline blue in 0.067 M phosphate buffer at pH 8.5 for 2 h and mounted in the stain (Ruzin, 1999). The fluorescence was observed under a LSM510 META confocal laser-scanning microscope (Carl Zeiss) with the filter combination of 350 nm exciter, and 460 nm barrier filter.

### Size determination of developing ovules

Measurements were made of the x (width) and y (length) axes of median sections of the megasporocyte and the developing embryo sac (a minimum of 20 ovules at each developing stage).

### Cryo-scanning electron microscopy

The developing nucellar filaments at the time of anthesis were dissected and loaded onto stubs. The samples were frozen by liquid nitrogen slush, and then transferred to the sample preparation chamber at -160°C. The samples were etched for 10 min at -85°C. After gold coating at -130°C, the samples were transferred to SEM and observed at -160°C with the cryo-scanning electron microscope (FEI Quanta 200 SEM, Quorum Cryo System PP2000TR FEI; FEI Company, Hillsboro, Oregon).

## RESULTS

The major post-pollination developmental events that occured in *P. delenatii* ovules are summarized in Table 1. At anthesis, the placental tissue within the ovary consisted of three ridges (Figure 1B). Each ridge had many highly branched nucellar filaments (Figures 1C and D) that consisted of approximately five to six nucellar cells that were covered by the nucellar epidermis. The nucellar cell located at the uppermost end (the tip end) of a nucellar filament just underneath the epidermis enlarged and differentiated into an archesporial cell (Figure 2A). Fifteen days after pollination (DAP), the archesporial cell enlarged further (Figure 2B) and differentiated into the megasporocyte. Prior to meiosis, the megasporocyte was distinguished by having an elongated cell axis. The nucleus was located at the micropylar end of the cell. Since the large nucleus was located at one end of the cell, the cytoplasm was displaced to the chalazal end of the megasporocyte. Starch granules were abundant within the chalazal cytoplasm at this time (Figure 2C). The integument elongated and gradually extended towards the tip of the nucellar filament (Figure 2C).

### Megasporogenesis

After 20 DAP, the first meiotic cell division created an unequal dyad (Figure 2D). The chalazal dyad was rich in cytoplasm with abundant starch grains present. The

**Table 1.** Major post-pollination developmental events occurring in *P. delenatii* ovules.

| DAP[a] | Developmental Satge |
|---|---|
| 0 | Archesporial cell |
| 15 | Megasporocyte |
| 20 | Functional dyad |
| 20-30 | 2-nucleate embryo sac |
| 30-40 | 4-nucleate embryo sac |
| 40-50 | Mature embryo sac |

[a] DAP = days after pollination.

micropylar dyad showed less staining in the cytoplasm; its nucleus rounded up with a denser appearance when compared to the nucleus of the chalazal dyad (Figure 2D). A distinct callose layer clearly separated the micropylar dyad from the chalazal one (Figure 3A). The functional dyad continued to enlarge in size, while the micropylar dyad became increasingly compressed (Table 2, Figure 2E). The nucleus of the functional dyad was large with a number of micro-nucleoli present. At that time, a callose wall completely enclosed the functional dyad (Figure 3B). The functional dyad continued to enlarge through the process of vacuolation (Figure 2F). As the functional dyad increased in size, the micropylar dyad became compressed and eventually, only the degenerating nucleus was visible (Figure 2F). As the functional dyad increased its size, the callose gradually disappeared from the lateral walls of the functional dyad; however, callose remained in the walls, especially in the common wall separating the two dyads as well as in the chalazal end wall of the functional dyad (Figure 3C). When comparing the size of the functional dyad to that of the megasporocyte, it was obvious that the former was slightly smaller than the latter (Table 2).

## Megagametogenesis

Between 20 to 30 DAP, the functional dyad underwent the second meiotic division (Figure 2G), forming a two-nucleate embryo sac directly (Figure 2H). Callose was no longer detectable in the walls of the developing embryo sac. Vacuolation of the embryo sac began as a large vacuole formed near the center of the cell (Figure 2I). It is important to note that more cytoplasm with an abundant

**Table 2.** Changes in cell dimensions during embryo sac development.

| Developmental stages | X-axis[a] | Y-axis[a] |
|---|---|---|
| Megasporocyte | 28.8 ± 1.2 | 50.4 ± 4.6 |
| Functional dyad | 26.2 ± 1.6 | 41.2 ± 5.2 |
| 2-nucleate embryo sac | 30.4 ± 2.9 | 52.5 ± 6.5 |
| 4-nucleate embryo sac | 55.4 ± 8.2 | 140.5 ± 16.2 |
| Mature embryo sac | 87.8 ± 15.3 | 252.2 ± 21.8 |

[a]X, Y standard deviation in μm.

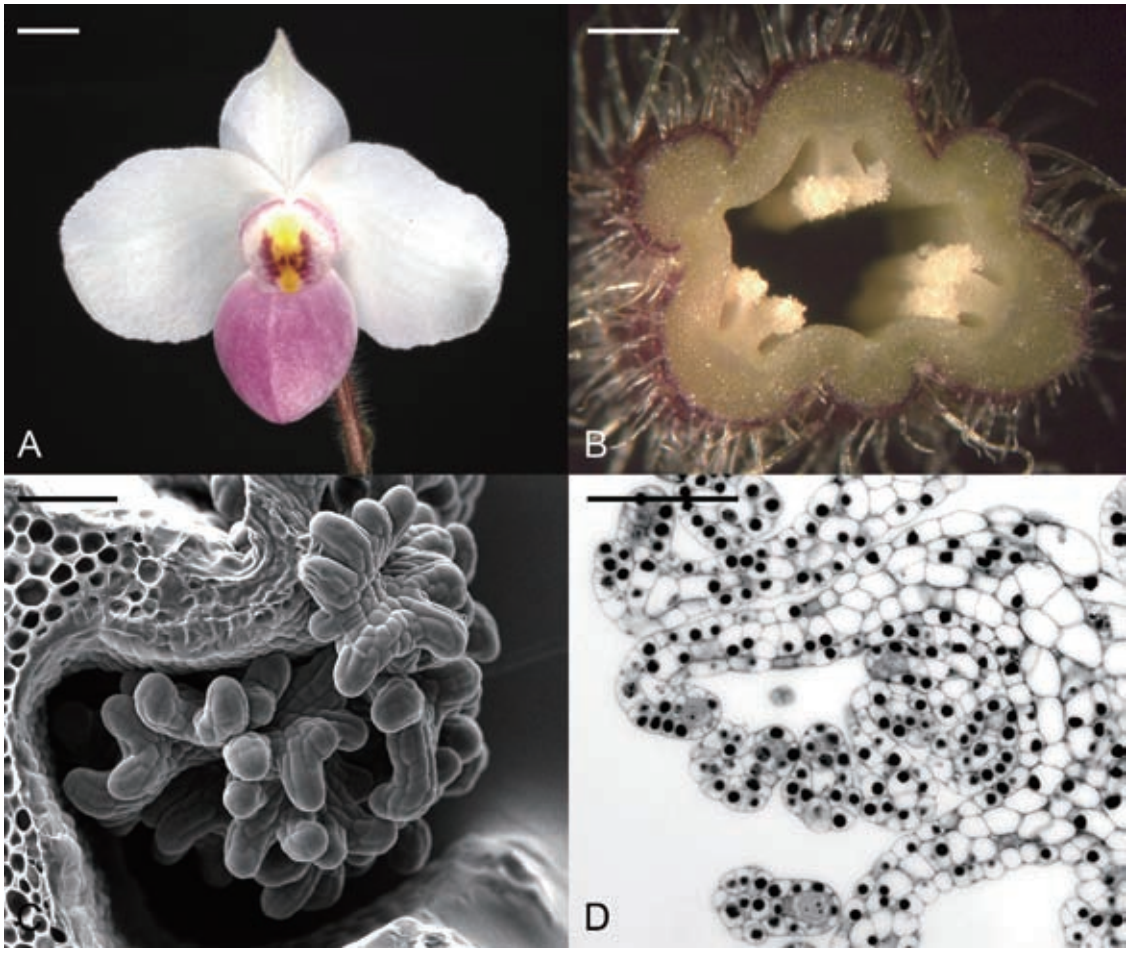


**Figure 1.** The flower and developing nucellar filaments in the ovary of *P. delenatii* at the time of anthesis. (A) The front view of flower at anthesis. Scale bar = 10 mm; (B) The ovary cross-section showing the 3-ridged placental tissue. Each ridge has many nucellar filaments (arrow). Scale bar = 2 mm; (C) The scanning electron microscope (SEM) micrograph of the highly branched nucellar filaments. Scale bar = 100 μm; (D) The historesin section of the nucellar filaments. Scale bar =100 μm.

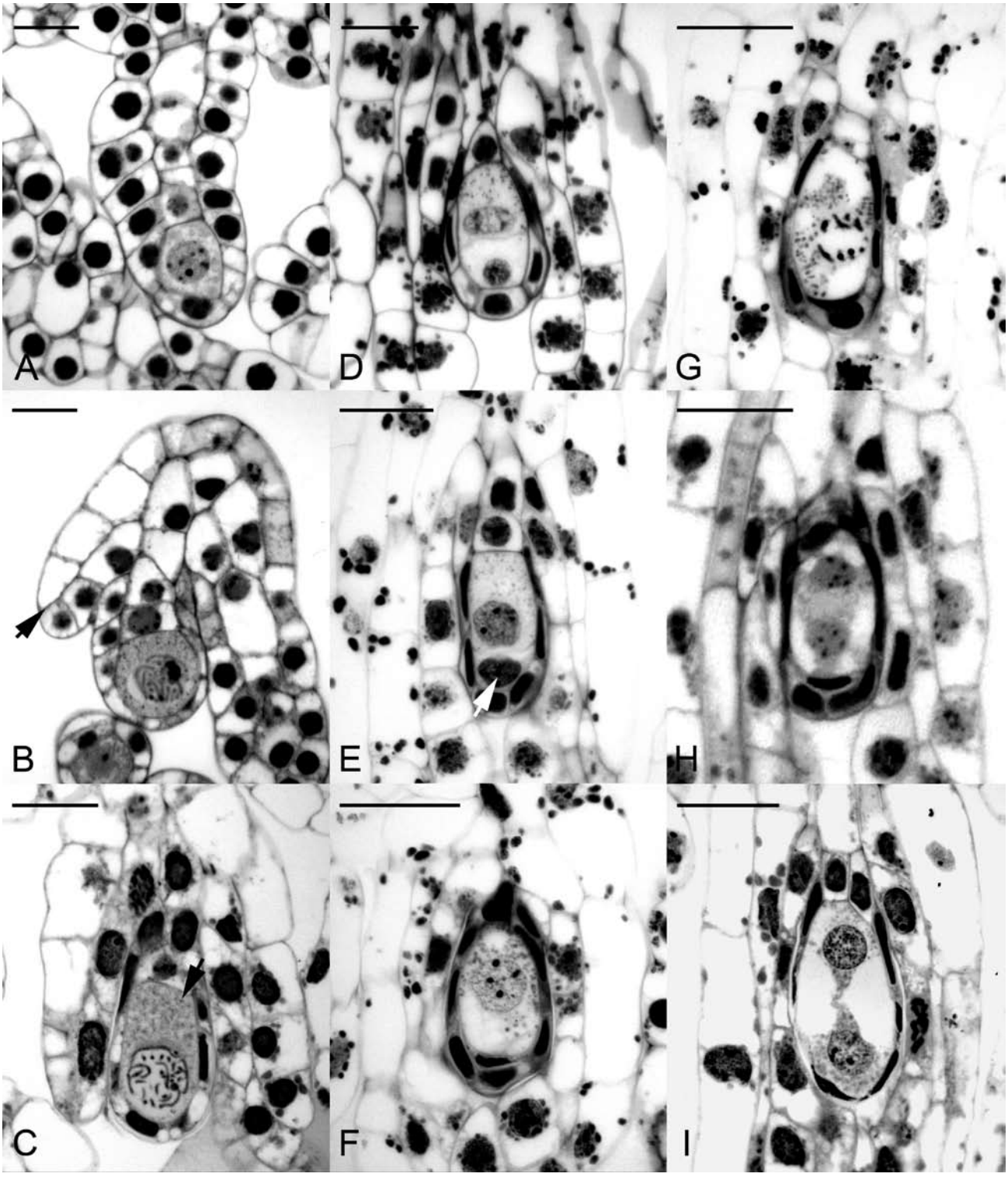


**Figure 2.** Light micrographs of megasporogenesis. (A) Archesporial cell (arrow) formation at the terminus of the nucellar filament. Scale bar = 20 μm; (B) The archesporial cell further enlarges and differentiates into the megasporocyte. As the archesporial cell differentiates, the integument tissues are initiated (arrow). Scale bar = 20 μm; (C) Elongation of megasporocyte before the first meiotic division. Starch grains accumulate at the chalazal end of the megasporocyte (arrow). Scale bar = 30 μm; (D) An unequal dyad resulting from the first meiotic division. Scale bar = 30 μm; (E) Light micrograph showing a functional chalazal dyad and a non-functional micropylar dyad that will gradually degenerate (arrow). Scale bar = 30 μm; (F) The functional chalazal dyad enlarges prior to the second meiotic division. Scale bar = 30 μm; (G) Light micrograph showing the second meiotic division as the chromosomes separate at the anaphase. Scale bar = 30 μm; (H) The second meiotic division results in the formation of a two-nucleate embryo sac. No cell wall is laid down between the nuclei within the chalazal dyad after the second meiotic division. Scale bar = 30 μm; (I) Vacuolation of the two-nucleate embryo sac begins as a large vacuole forms near the center of the cell. Scale bar = 30 μm.

starch deposit was present at the micropylar end of the cell where the egg apparatus would eventually form (Figure 2I). The two-nucleate embryo sac expanded remarkably (Table 2, Figure 4A). A subsequent division of the two-nucleate embryo sac (Figure 4B) resulted in the formation of a four-nucleate embryo sac during 30 to 40 DAP. The nuclei were of similar size at the four-nucleate stage and a large vacuole occupied the center of the embryo sac (Figure 4C). Only the micropylar nuclei of the four-nucleate embryo sac (Figure 4D) divided again and would produce a six-nucleate embryo sac. In a mature embryo sac, the egg apparatus contained the egg cell and two synergids and was located at the micropylar end with a prominent filiform apparatus (Figure 4E). There was a considerable increase in embryo sac size from the four-nucleate stage to the mature embryo sac stage during 40 to 50 DAP (Table 2). As the embryo sac matured and expanded, its nucellar epidermis stretched. The embryo sac contents were presumably absorbed by the expanding embryo sac and were barely detectable. After fertilization, the zygote contained a large vacuole at the micropylar end; and one of the synergids degenerated (Figure 4G).

The appearance of Nile red positive material was stage specific. Nile red staining was absent from the developing embryo sac until the formation of the egg apparatus. The lipidic material was present in the innermost walls of the embryo sac and appeared as a dense red line. Judging from its location, it was presumed to be cuticular material. This substance started to accumulate and presented in the lateral walls of the embryo sac as it reached maturity (Figure 4F). After fertilization, the intensity of the staining increased further (Figure 4H).

### The integuments

The integument tissue was initiated at the time of archesporial cell formation. It appeared as a small projection at the base of the nucellar filament (Figure 2B). As the megaspore underwent meiosis, the integument tissue continued to extend toward the tip of the nucellar filament (Figures 2D to G); eventually the integument enclosed the developing embryo sac, leaving a micropyle. During these stages, three cell layers of the integument were discriminated: the cells of the outer two layers were larger and highly vacuolated, while the innermost layer was composed of smaller cells with dense cytoplasm.

## DISCUSION

Similar to other *Paphiopedilum* species studied, *P. delenatii* has a bisporic pattern of embryo sac development with a cell number reduction in a mature embryo sac. Using current histological methods, we observed several notable cytological changes during the course of embryo sac formation, i.e. (1) the uneven distribution of the cytoplasm and starch granules, (2) the changing callose deposition pattern during the course of megasporogenesis, and (3) the presence of a cuticle partially surrounding the maturing embryo sac.

At the early megasporocyte stage in *P. delenatii*, the nucleus is centrally located and the cytoplasm is evenly distributed around it (Figures 2A and B). As the megasporocyte enlarges, the nucleus relocates to the micropylar end of the cell displacing the cytoplasm to the chalazal end. As a result, the dyads have different cytoplasmic contents after the first meiotic division. The difference

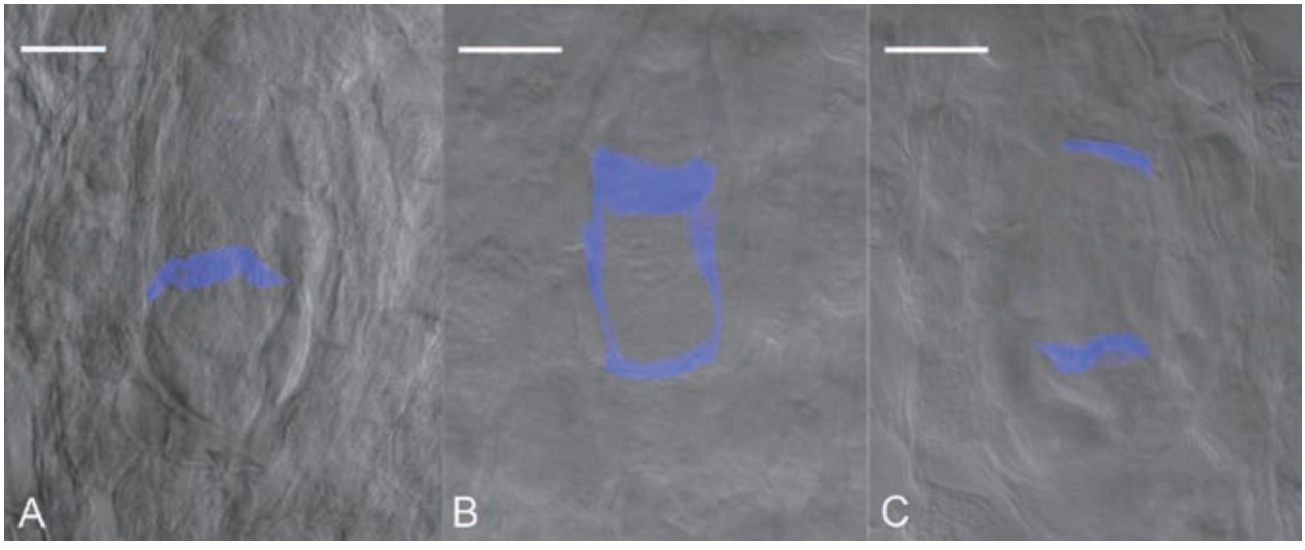


**Figure 3.** Light micrographs showing the callose deposition. (A) Callose is first detected in the common wall separating the members of the dyad. Scale bar = 15 μm; (B) Later than, callose completely surrounds the functional chalazal dyad, isolating the functional chalazal dyad from the degenerating micropylar dyad. Scale bar = 15 μm; (C) As the functional chalazal dyad continues to enlarge, callose can only be detected in the common wall separating the two dyads and in the chalazal end wall of the functional dyad. Scale bar = 15 μm.

in cytoplasmic content between the two cells most likely leads to the different fates observed. The polarization of cytoplasmic components has been reported in many flowering plants (Yeung and Law, 1997). In *P. spicerianum*, a polarized distribution has also been reported (Corti and Cecchi, 1970). In *Cyripedium passerinum*, a temperate slipper orchid species with a bisporic development, a highly polarized cytoplasm is also observed with a large number of starch granules located at the chalazal end of the megasporocyte (Law and Yeung, 1993). In this study, the polarized cytoplasm may be due to a more active synthesis and accumulation of nutrients at the chalazal end of the megasporocyte. Nutrients have to come from the adjoining nucellar cells of the nucellar filament. The resulting accumulation of cytoplasm may "push" the nucleus towards the micropylar end of the cell. Since organelles are not statically localized, it would be interesting to determine whether the cytoskeletal elements, i.e. microtubules and microfilaments play a role in localizing the nucleus within the megasporocyte at the time of the first meiotic division (Zee and Ye, 1995; Ye et al., 1996).

Callose deposition is common in cells undergoing meiotic divisions (Rodkiewicz, 1970). During pollen development, the microsporocytes are distinctly enclosed

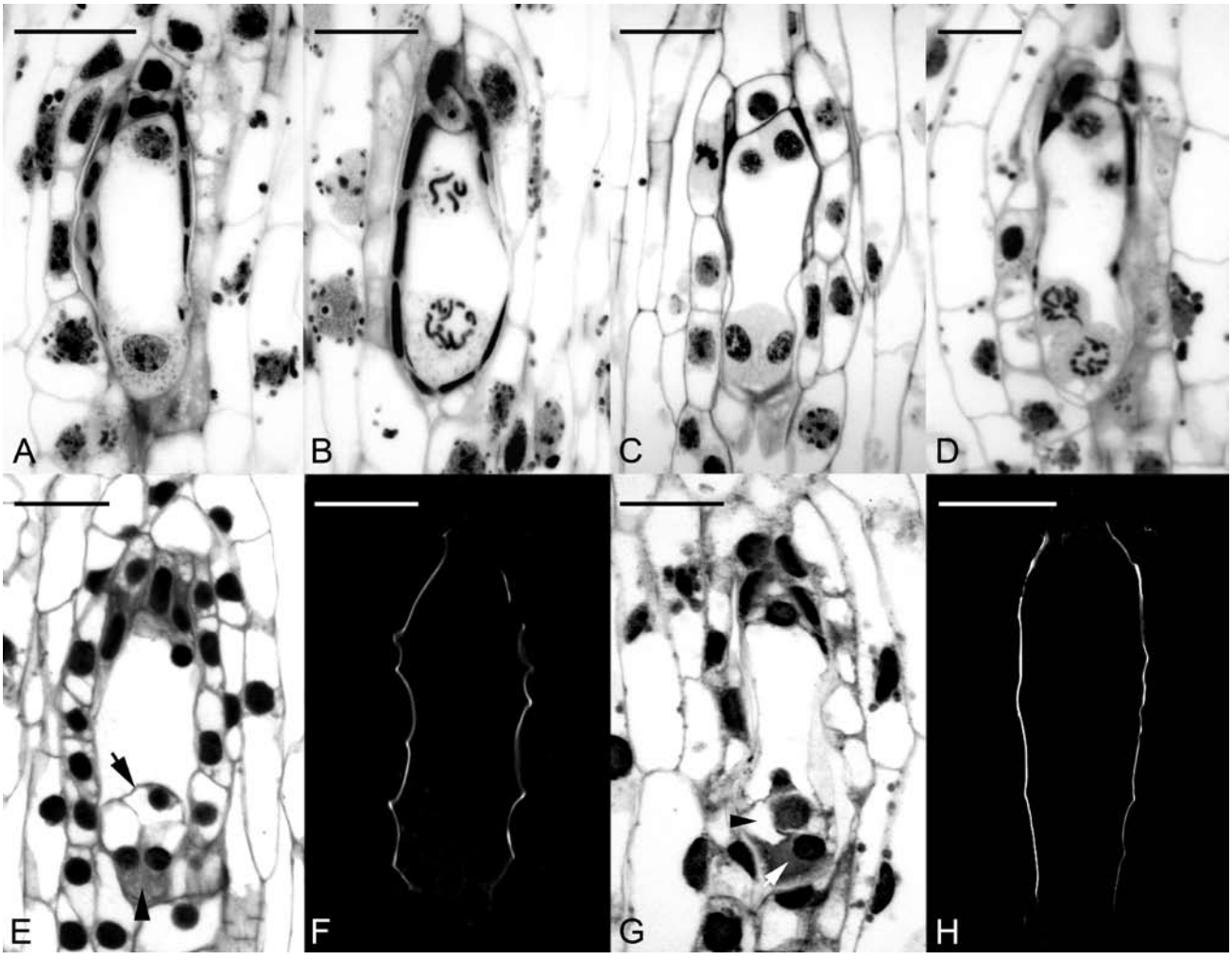


**Figure 4.** Light micrographs of megagametogenesis. (A) The large central vacuole aids in the rapid expansion of the two-nucleate embryo sac. Scale bar = 30 μm; (B) Light micrograph showing a two-nucleate embryo sac undergoing the first mitotic cell division, resulting in the formation of a four- nucleate embryo sac. Scale bar = 30 μm; (C) Light micrograph showing a four-nucleate embryo sac with similar nucleus size. Scale bar = 50 μm; (D) Only the micropylar nuclei of the four-nucleate embryo sac divide again to produce a six-nucleate embryo sac. Scale bar = 50 μm; (E) A mature embryo sac showing the egg apparatus, including the egg cell (arrow) and two synergids with a prominent filiform apparatus (arrowhead). Scale bar = 80 μm; (F) Nile red staining fluorescence micrograph of a mature embryo sac at the same stage as that seen in Fig. 3E. The fluorescence outline is first detected in the innermost walls of the innermost layer of the integument as the embryo sac reaches maturity. Scale bar = 80 μm; (G) Light micrograph of a zygote (arrowhead) just after fertilization at 60 DAP. The zygote is polarized with a chalazally-located nucleus and a prominent vacuole occupying the micropylar end. The arrow indicates the degenerated synergid. Scale bar = 80 μm; (H) Nile red staining fluorescence micrograph of a zygote stage similar to Figure 3G. The innermost walls of the innermost layer of the seed coat fluoresce brightly. Note the lack of wall fluorescence near both the chalazal and micropylar ends. Scale bar = 80 μm.

by a callosic wall. Although callose is present in the wall at some stages of meiotic division in the megasporocyte, the pattern of callose deposition varies. In the majority of examples having a monosporic pattern of embryo sac formation, callose deposition is found at the megasporocyte stage (Law and Yeung, 1989; Yeung and Law, 1989). In the bisporic mode of embryo sac formation, for the few examples reported (Law and Yeung, 1993; Yeung et al., 1994), callose is absent from the megasporocyte but becomes distinct after the first meiotic division. Does this pattern of callose deposition ensure a bisporic pattern of embryo sac formation? Often, the callose staining is based on sectioned material. The sections can be very thin, and callose detection becomes more difficult. In this study, whole-mount staining was used. This method of staining allowed for better visualization of the callose present. The intense staining between the functional and the non-functional dyad was a common observation reported in the literature (Yeung and Law, 1997) and most likely served to block off or reduce communication between the cells, as they had different cell fates. However, the intense staining at the chalazal wall from the functional dyad appeared to be unique to the bisporic mode of embryo sac development. Callose deposition during microspore development severed symplastic communications between pollen tetrads. If the same principle applied, the presence of callose deposition in the chalazal wall would have severed symplastic connections between the functional dyad and the nucellar cells. This interruption may be necessary for the functional dyad to complete the second meiotic division leading to the formation of a bisporic type of embryo sac.

One of the most notable findings in this study was the presence of cuticular substance in the wall of the embryo sac at the time near its maturation. Fluorescence was absent from a 4-nucleate embryo sac and was first detected as the embryo sac reached maturity. Figures 4F and H clearly indicate that fluorescence was present in the lateral walls but was absent in the walls of both the chalazal and micropylar ends of the embryo sac. The lack of cuticular deposits at the chalazal end ensured continual nutrient flow from the maternal tissues. The lack of cuticular deposits at the micropylar end ensured that the entrance of the pollen tube was not going to be interrupted. The deposition of the cuticular material may serve other purposes. It is interesting to note that the size of embryo sac in *P. delenatii* was fairly large when compared with other epiphytic orchid species (Yeung and Law, 1997). The cuticular material may function to strengthen the embryo sac. After fertilization, the cuticular layer helped to conserve water within the seed as the embryo developed.

This structural study identifies a number of interesting features during ovule development in *P. delenatii*. The relatively large size and the numerous ovules present within a single ovary will enable us to study the cell biology of bisporic embryo sac development in the future.

**Acknowledgement.** We thank Dr. Mei-Chu Chung in Institute of Plant and Microbial Biology, Academia Sinica, Taipei Taiwan (IPMB), and Dr. Wann-Neng Jane and Miss Mei-Jane Fang (Plant Cell Biology Core lab, IPMB) for the use of a confocal laser-scanning microscope and a cryo-scanning electron microscopy. This research was supported by a Discovery grant from the Natural Sciences and Engineering Research Council of Canada to E.C. Yeung, and by grants from the National Museum of Natural Science to Yung-I Lee.

## LITERATURE CITED

Arditti, J. 1992. Fundamentals of Orchid Biology. John Wiley and Sons, Inc., New York.

Averyanov, L., P. Cribb, P.K. Loc, and N.T. Hiep. 2003. Slipper Orchids of Vietnam. Compass Press Limited, The Royal Botanic Gardens, Kew, UK.

Cribb, P. 1998. The genus *Paphiopedilum*, 2nd ed. Natural History Publications, Kota Kinabalu, Sabah and The Royal Botanic Gardens, Kew, UK.

Carlson, M.C. 1945. Megasporogenesis and development of the embryo sac of *Cypripedium parviflorum*. Bot. Gaz. **107:** 107-114.

Corti, E.F. and A.F. Cecchi. 1970. The behaviour of the cytoplasm during the megasporogenesis in *Paphiopedilum spicerianum* (Rchb. F.) Pfizer. Caryologia **23:** 715-727.

Duncan, R.E. and J.T. Curtis. 1942. Intermittent growth of fruits of *Cypripedium* and *Paphiopedilum*. A correlation of the growth of orchid fruits with their internal development. Bull. Torrey Bot. Club **69:** 353-359.

Law, S.K. and E.C. Yeung. 1989. Embryology of *Calypso bulbosa*. I. Ovule development. Am. J. Bot. **76:** 1668-1674.

Law, S.K. and E.C. Yeung. 1993. Embryology of *Cypripedium passerinum* (Orchidaceae): ovule development. Lindleyana **8:** 139-147.

Lee, Y.I., E.C. Yeung, N. Lee, and M.C. Chung. 2006. Embryo development in the lady's slipper orchid, *Paphiopedilum delenatii* with emphases on the ultrastructure of the suspensor. Ann. Bot. **98:** 1311-1319.

Relser, L. and R.L. Fischer. 1993. The ovule and the embryo sac. Plant Cell **5:** 1291-1301.

Rodkiewicz, B. 1970. Callose in cell walls during megasporogenesis in angiosperm. Planta **93:** 39-47.

Ruzin, S.E. 1999. Plant microtechnique and microscopy. Oxford Universivty Pree, Inc., New York.

Swamy, B.G.L. 1943. Embryology of Orchidaceae. Curr. Sci. **12:** 13-17.

Vij, S.P. and M. Sharma. 1986. Embryo sac development in Orchidaceae. *In* S.P. Vij (ed.), Biology, conservation, and culture of orchids. East-West Press, New Delhi, pp. 31-48.

Wirth, M. and C.L. Withner. 1959. Embryology and development in the Orchidaceae. *In* C.L. Withner (ed.), The Orchids: A Scientific Survey. Ronald Press, New York, pp. 155-188.

Ye, X.L., E.C. Yeung, S.Y. Zee, and S.H. Tong. 1996. Confo-

cal microscopic observation on microtubular cytoskeleton changes during megasporogenesis and megagametogenesis in Nun orchid, *Phaius tankervilleae* (Aiton) Bl. Acta Bot. Sin. **38:** 677-685.

Yeung, E.C. 1984. Histological and histochemical staining procedures. *In* I.K. Vasil, (ed.), Cell Culture and Somatic Cell Genetics of Plants. Academic Press, Orlando, pp. 689-697.

Yeung, E.C. 1999. The use of histology in the study of plant tissue culture systems - some practical comments. In Vitro Cell. Dev. Biol.- Plant **35:** 137-143.

Yeung, E.C. and S.K. Law. 1989. Embryology of *Epidendrum ibaguense*. I. Ovule development. Can. J. Bot. **67:** 2219-2226.

Yeung, E.C. and S.K. Law. 1997. Ovule development. *In* J. Arditti and A.M. Pridgeon (eds.), Orchid Biology: Reviews and Perspectives VII. Kluwer Academic Pub., Dordrecht, pp. 31-73.

Yeung, E.C., S.Y. Zee, and X.L. Ye. 1994. Embryology of *Cymbidium sinense*: ovule development. Phytomorphology **44:** 55-63.

Zhang, X.S. and S.D. O'Neill. 1993. Ovary and gametophyte development are coordinately regulated by auxin and ethylene following pollination. Plant Cell **5:** 403-418.

Zee, S.Y. and X.L. Ye. 1995. Changes in pattern of organization of microtubular cytoskeleton during megasporogenesis in *Cymbidium sinense*. Protoplasma **185:** 170-177.

# 仙履蘭之胚胎學研究：胚囊發育

李勇毅[1] Edward C. YEUNG[2]

[1] 國立自然科學博物館 植物學組

[2]Department of Biological Sciences, University of Calgary, Calgary, Alberta T2N 1N4, Canada

仙履蘭 (*Paphiopedilum delenatii*) 為原生於越南的瀕危蘭花物種，具有極高的觀賞價值。深入研究瀕危物種的生殖生物學將有助於推展繁殖與保育工作之規劃。仙履蘭之胚囊發育為雙孢型，成熟的胚囊具有六細胞。在授粉前，珠心絲構造已存於子房內。授粉後 15 天，位於珠心絲頂端的孢原細胞分化成大孢子母細胞。當大孢子母細胞成熟時，其細胞核坐落於近珠孔端；如此使得大孢子母細胞的細胞質呈不均勻分布，富含澱粉粒的細胞質則較集中於合點端。第一次減數分裂後，明顯的胼胝質層將二分子隔開 : 一個近珠孔，另一個近合點。接著，靠近合點而具有功能的二分子被胼胝質完全包圍。當具有功能的二分子擴張，胼胝質此時累積於二分子之共同細胞壁，以及近合點端之細胞壁。本研究另一值得注意的觀察結果 : 仙履蘭成熟胚囊之兩側細胞壁具有角質之累積。由於仙履蘭胚囊的體積相當大，累積角質可能提供胚囊細胞壁支撐，並且在受精後保持胚囊內之水分以助後續之胚胎發育。

**關鍵詞：**胼胝質；胚胎學；仙履蘭；尼羅紅；胚珠。